JACS
JOURNAL OF THE AMERICAN CHEMICAL SOCIETY
Article
pubs.acs.org/JACS

Inhibition of Mucin-Type *O*-Glycosylation through Metabolic Processing and Incorporation of *N*-Thioglycolyl-D-galactosamine Peracetate (Ac_5GalNTGc)

Kavita Agarwal, Rachna Kaul, Monika Garg, Asif Shajahan, Saroj Kumar Jha, and Srinivasa-Gopalan Sampathkumar*

Laboratory of Chemical Glycobiology (CGB), National Institute of Immunology (NII), Aruna Asaf Ali Marg, New Delhi 110067, India

Supporting Information

ABSTRACT: Mucin-type *O*-glycans form one of the most abundant and complex post-translational modifications (PTM) on cell surface proteins that govern adhesion, migration, and trafficking of hematopoietic cells. Development of targeted approaches to probe functions of *O*-glycans is at an early stage. Among several approaches, small molecules with unique chemical functional groups that could modulate glycan biosynthesis form a critical tool. Herein, we show that metabolism of peracetyl *N*-acyl-D-galactosamine derivatives carrying an *N*-thioglycolyl (Ac_5GalNTGc, **1**) moiety—but not *N*-glycolyl (Ac_5GalNGc, **2**) and *N*-acetyl (Ac_4GalNAc, **3**)—through the *N*-acetyl-D-galactosamine (GalNAc) salvage pathway induced abrogation of MAL-II and PNA epitopes in Jurkat cells. Mass spectrometry of permethylated *O*-glycans from Jurkat cells confirmed the presence of significant amounts of elaborated *O*-glycans (sialyl-T and disialyl-T) which were inhibited upon treatment with **1**. *O*-Glycosylation of CD43, a cell surface antigen rich in *O*-glycans, was drastically reduced by **1** in a thiol-dependent manner. By contrast, only mild effects were observed for CD45 glycoforms. Direct metabolic incorporation of **1** was confirmed by thiol-selective Michael addition reaction of immunoprecipitated CD43-myc/FLAG. Mechanistically, CD43 glycoforms were unperturbed by peracetylated *N*-(3-acetylthiopropanoyl) (**4**), *N*-(4-acetylthiobutanoyl) (**5**), and *N*-methylthioacetyl (**6**) galactosamine derivatives, *N*-thioglycolyl-D-glucosamine (**7**, C-4 epimer of **1**), and *α*-*O*-benzyl 2-acetamido-2-deoxy-D-galactopyranoside (**8**), confirming the critical requirement of both free sulfhydryl and galactosamine moieties for inhibition of mucin-type *O*-glycans. Similar, yet differential, effects of **1** were observed for CD43 glycoforms in multiple hematopoietic cells. Development of small molecules that could alter glycan patterns in an antigen-selective and cell-type selective manner might provide avenues for understanding biological functions of glycans.

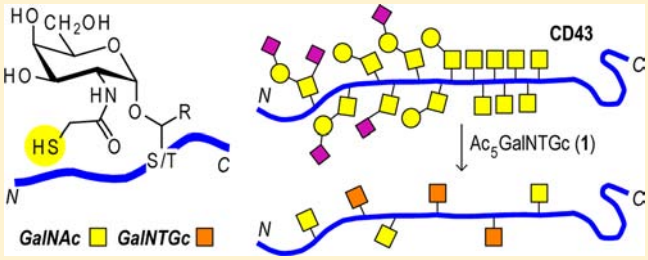

INTRODUCTION

Investigation of structure and function of *O*-linked glycans presents additional challenges compared to *N*-linked glycans, due to the presence of multiple initiating monosaccharide building blocks and variety of core structures coupled with lack of consensus sequons, specific biochemical tools, and inhibitors.[1] Among various types of glycosylations, mucin-type *O*-glycosylation constitutes one of the most abundant on mammalian cell surface.[2,3] Biosynthesis of mucin-type *O*-glycans is initiated by the addition of GalNAc to Ser/Thr by UDP-GalNAc:polypeptide *N*-acetyl-galactosaminyl-transferases (ppGalNAcT).[4−6] *α*-*O*-GalNAc-S/T (Tn-antigen) is elaborated by addition of Gal, GlcNAc, Fuc, and NeuAc to yield a variety of complex glycan structures exquisitely orchestrated by a battery of respective glycosyl transferases. Multiple approaches could be envisaged for elucidation of glycan-dependent functions each with unique merits and limitations: (i) glycoprotein specific knockout models lead to loss of both protein and its glycans;[7] (ii) knockouts of specific glycosyl transferases results in simultaneous perturbation of multiple protein substrates;[8,9] (iii) efficient *O*-glycan inhibitors, despite the drug development potential,[10] have been few and far between with most compounds focused mostly on substrate decoys and uridine analogues;[11−13] and (iv) installation of monosaccharide building blocks carrying non-natural functional groups enabling bio-orthogonal ligation.[14]

Particularly, metabolic glycan engineering (MGE) methodology has been employed successfully for expression of non-natural carbohydrates on glycans exploiting the permissivity of glycosylation and salvage pathways (e.g., sialylation, fucosylation, mucin-type *O*-glycosylation, and *β*-*O*-GlcNAc) using peracetylated monosaccharide precursors.[15−18] Peracetylated *N*-azidoacetyl-D-galactosamine (Ac_4GalNAz) and *N*-glycolyl-D-galactosamine (Ac_5GalNGc) are readily metabolized through the GalNAc salvage pathway and incorporated into mucin-type

Received: May 23, 2013
Published: August 29, 2013

dx.doi.org/10.1021/ja405189k | J. Am. Chem. Soc. 2013, 135, 14189−14197

O-glycans both *in vitro* and *in vivo*.[19−21] Peracetylated non-natural GalNAc analogues (GalNR) are first deacetylated intracellularly, converted to UDP-GalNR *via* GalNR-1-P, and then transported to ER/Golgi for utilization by ppGalNAcTs.[19]

On one hand, MGE has been exploited for direct incorporation and imaging of glycans.[17] On the other hand, depending on the specific chemical structure, metabolism of non-natural analogues is likely to exhibit altered affinities and reaction rates for glycosylation pathway enzymes with respect to wild-type substrates. Kinetic studies have shown that UDP-GalNAz is utilized at one-third the rate as compared to UDP-GalNAc by ppGalNAcTs.[22] *In vivo* usage of peracetyl 2-acetamido-2,4-dideoxy-4-fluoro-D-galactosamine (Ac_3-4F-GalNAc) has been shown to inhibit elaboration of *O*-glycans *via* metabolic incorporation in P-selectin glycoprotein ligand-1 (PSGL-1/CD162) and modulate leukocyte adhesion.[23] Other *in vitro* studies using non-natural UDP-GalNAc analogues as donors and recombinant MUC1 protein as an acceptor have shown that relative incorporation of non-natural epitopes are governed by both size and nature of functional groups.[24,25] Typically, the trade-off for metabolic processing of non-natural monosaccharide analogues is an alteration to the full complement of cellular glycosylation patterns.

In this context, we wanted to investigate whether non-natural GalNAc analogues could be utilized as tools to alter the overall carbohydrate-loading and pattern of mucin-type *O*-glycosylation, exploiting MGE. We surmised that, depending on the chemical nature of the non-natural functional group and possible utilization of UDP-GalNR (R = acyl) as donors by ppGalNAcTs, the result might be direct incorporation, which in turn might attenuate subsequent elaboration of *O*-glycans and neighbor site decoration. Herein, we show thiol-specific effects on selective inhibition of *O*-glycosylation both globally and in selected lymphocyte cell surface antigens induced by peracetyl *N*-thioglycolyl-D-galactosamine (Ac_5GalNTGc, **1**).[26] A panel of peracetylated *N*-acyl-D-galactosamine derivatives carrying *N*-glycolyl (Ac_5GalNGc, **2**),[21] *N*-acetyl (Ac_4GalNAc, **3**), *N*-(3-acetylthiopropanoyl) (Ac_5GalNTPr, **4**), *N*-(4-acetylthio-butanoyl) (Ac_5GalNTBut, **5**), and *N*-methylthioacetyl (Ac_4GalNMeTA, **6**) were synthesized (Figure 1A) (Supporting Information). Additionally, peracetyl *N*-thioglycolyl-D-glucosamine (Ac_5GlcNTGc, **7**—C-4 epimer of **1**),[26] peracetyl benzyl 2-acetamido-2-deoxy-α-D-galactopyranoside (Ac_3-α-BnGalNAc, **8**),[27] and nonacetylated α-*O*-BnGalNAc (**9**) were employed as controls. Metabolic processing of **1** *via* GalNAc salvage pathway (Figure 1B) specifically induced drastic hypoglycosylation of CD43 (leukosialin/sialophorin) in Jurkat (human T-cell leukemia) cells as a consequence of direct incorporation. We show for the first time that, depending on the nature of the installed chemical moiety, non-natural GalNAc analogues drastically affect mucin-type *O*-glycosylation. These small molecules act as a first step in manipulating mucin-type *O*-glycans and may further serve as valuable probes in probing the relationship between structure and function of mucins in biological processes.

RESULTS AND DISCUSSION

Metabolic effects of non-natural monosaccharide analogues on glycosylation may be broadly classified into three categories: (i) incorporation with minimal effects on overall glycan structures,[15,20,28] (ii) altered glycan structures with no incorporation,[29−32] and (iii) altered glycan structures as a consequence of metabolic incorporation.[23] Due to the specific

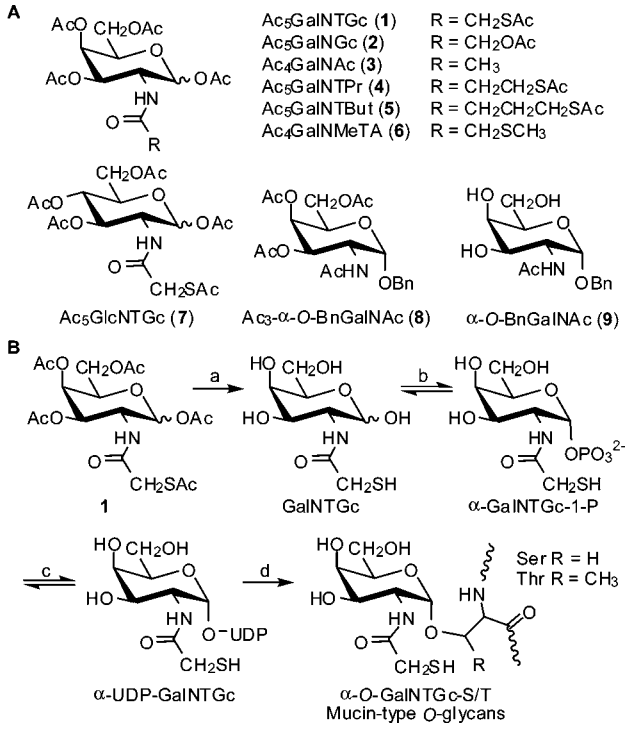

Figure 1. Metabolic processing through the GalNAc salvage pathway. (A) Structures of peracetylated GalNAc analogues **1**−**8** and **9**. (B) Biosynthetic processing of **1** by (a) intracellular esterases, (b) GalNAc-1-kinase, (c) UDP-GalNAc pyrophosphorylase, and (d) polypeptide *N*-acetylgalactosaminyltransferases (ppGalNAcT) results in expression of thiol functionality on Tn-antigen, the initiating monosaccharide for biosynthesis of mucin-type *O*-glycans.

chemical properties of the sulfhydryl group, metabolism of **1** was anticipated to impact mucin-type *O*-glycan biosynthesis in a unique manner. We chose Jurkat cells as a model, as earlier studies have shown that **1** is metabolized readily resulting in a 2.5-fold increase in accessible cell surface thiol (CST) levels.[26] The oxa analogue **2** and analogue **3** (a precursor for "natural" GalNAc) were used as controls for effects due to intracellular deacetylation and altered metabolic flux in the GalNAc salvage and mucin-type *O*-glycosylation pathways.

Disrupting the Sugar Coat: Metabolic Processing of 1, but Not 2, Abrogates MAL-II and PNA Epitopes in Jurkat Cells. In order to investigate whether GalNAc analogues affected overall cell surface glycosylation, we employed lectin staining.[33] Three lectins, namely, *Maackia amurensis* lectin-II (MAL-II) (binds to NeuAcα(2→3)Gal), *Sambucus nigra* agglutinin (SNA) (binds to NeuAcα(2→6)Gal/GalNAc), and peanut agglutinin (PNA) (binds to Galβ(1→3)GalNAc-S/T, also known as T-antigen and Thomson−Friedenreich (TF)-antigen) were used. Jurkat cells were incubated with dimethyl sulfoxide (DMSO, **D**) (vehicle), **2**, or **1** (100 μM, 48 h), treated without and with neuraminidase (*Neu*), stained with biotinylated lectins followed by AlexaFluor594-conjugated streptavidin, and studied by confocal imaging. Remarkably, binding of MAL-II was abrogated upon incubation with **1**, but not **D** or **2**, indicating thiol-specific effects. Expectedly, treatment with *Neu* resulted in loss of both MAL-II (Figure 2A) and SNA binding (Supporting Information Figure S1). SNA staining remained unaffected upon incubation with **D**, **2**, or **1** (Supporting Information Figure S1). No binding of peanut agglutinin (PNA) was detected on cells treated with **D**, **2**, or **1**, as PNA

dx.doi.org/10.1021/ja405189k | J. Am. Chem. Soc. 2013, 135, 14189−14197

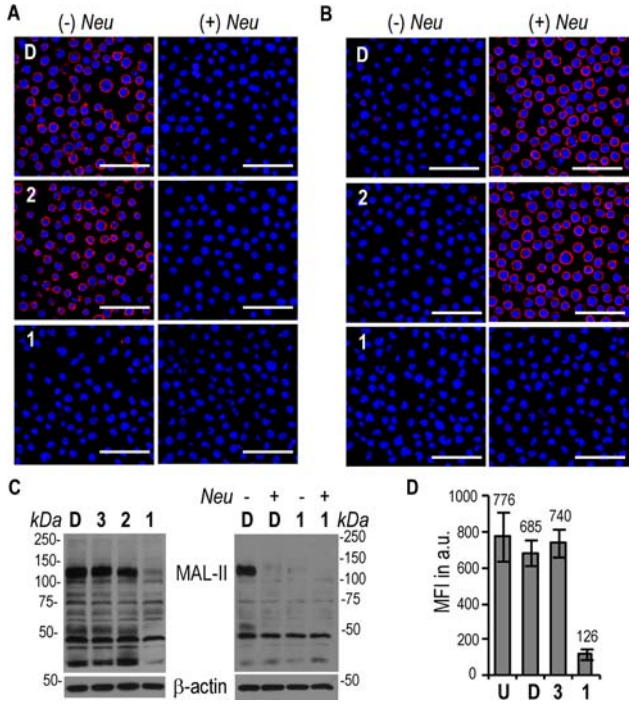

Figure 2. Thiol-dependent inhibition of expression of MAL-II and PNA epitopes in Jurkat cells induced specifically by **1**. Confocal imaging of cells incubated with **D**, **2**, or **1** (100 μM, 48 h), treated without and with *Neu*, fixed and stained with biotinylated lectins, (A) MAL-II and (B) PNA followed by AlexaFluor-594-conjugated streptavidin (red) and DAPI (blue). Images shown are representative of multiple field views of two replicate samples; scale bar = 50 μm. (C) MAL-II lectin blots of total lysates of cells incubated with **D**, **3**, **2**, or **1** (100 μM, 60 h) (left panel) and cells incubated with **D** or **1** (100 μM, 48 h) followed by treatment with and without *Neu* (right panel); β-actin blots are shown as loading controls. (D) Flow cytometry estimation of PNA binding in cells incubated with no vehicle (U), **D**, **3**, or **1** (50 μM, 48 h) and subjected to *Neu* treatment. MFI values are shown on the graph. Error bars shown are standard deviation of two replicate samples. **D**, DMSO; *Neu*, neuraminidase; U, untreated; MAL-II, *Maackia amurensis* lectin-II, PNA, peanut agglutinin, MFI in a.u., mean fluorescence intensity in arbitrary units.

epitopes are known to be masked by terminal sialylation. While cells treated with **D** or **2** revealed PNA epitopes after *Neu* treatment, strikingly, cells treated with **1** showed no PNA binding (Figure 2B). Absence of PNA binding in cells incubated with **1** even after *Neu* treatment suggested thiol-specific abrogation of T-antigens.

Lectin blots of total lysates of Jurkat cells incubated with **D**, **1**, **2**, or **3** clearly showed thiol-specific inhibition of MAL-II epitopes (Figure 2C). MAL-II binding was observed as prominent bands between 150 and 100 kDa in all cases except in cells treated with **1**. Interestingly the bands at 150−100 kDa coincide with apparent molecular weights of CD43 and CD162/PSGL-1, two major cell surface antigens on T-cells that are rich in *O*-glycans.[34,35] *Neu* treatment of cells incubated with **D** prior to lysis clearly showed loss of MAL-II epitopes, whereas MAL-II epitopes were absent in cells treated with **1** even without Neu treatment (Figure 2C). Notably, effects observed in MAL-II blots complement microscopy results and confirm absence of sialyl-T-antigen structures induced specifically by **1**.

Corroboration of thiol-specific inhibition of T-antigen was obtained by flow cytometry estimation of PNA binding to Jurkat cells incubated with no vehicle (U), **D**, **1**, or **3** for 48 h and subjected to *Neu* treatment (Figure 2D). PNA binding was similar in all cases (100% for untreated; 88% and 95% for cells treated with **D** and **3**, respectively) except in cells treated with **1** (16% of control), which suggested inhibition of T-antigen structures on cell surface by **1**. PNA binding to cells incubated with no vehicle (U), **D**, **3**, or **1**, that were not subjected to *Neu* treatment showed a similar pattern (Supporting Information Figure S2). We tested the possibility that abrogation of lectin binding could be a consequence of non-natural disulfides formed due to expression GalNTGc. Jurkat cells incubated with and without **1** (100 μM, 48 h) followed by treatment with tris(2-carboxyethyl)phosphine hydrochloride (TCEP) and maleimide-PEG_2-biotin (MB) showed no change in levels of PNA binding, confirming that reduction in PNA binding induced by **1** is indeed a consequence of *O*-glycan inhibition, and ruled out disulfide mediated changes to PNA binding (Supporting Information Figure S2). Specificity of PNA binding to T-antigen epitopes was confirmed by titration with its competitive ligand lactose (Supporting Information Figure S2).

Jurkat cells are generally considered to express low levels of elaborated *O*-glycans relative to K562 (human chronic myeloid leukemia)[36] and HL-60 (human acute myeloid leukemia).[35] This is attributed to (i) a mutation in *cosmc* (core1 beta3-Gal-T-specific molecular chaperone), a chaperone essential for proper folding and activity of T-synthase (glycoprotein-*N*-acetylgalactosamine 3-β-galactosyltransferase, C1GALT),[37] and (ii) absence of branched core2 glycans.[34] Surprisingly, Jurkat cells (untreated) showed a 13-fold gain in PNA binding upon *Neu* treatment (mean fluorescence intensity (MFI) of 60 arbitrary units (a.u.) without *Neu* and 776 a.u. with *Neu*) (Supporting Information Figure S2). Significant PNA binding observed by both confocal imaging and flow cytometry indicated that Jurkat cells, nonetheless, do express substantial levels of T-antigen structures.

In order to test if the thiol-specific effects observed with **1** were caused by cytotoxicity, a viability assay using propidium iodide (PI) and annexin-V was performed (Supporting Information Figure S3). Jurkat cells treated with **D**, **2**, and **1**, were found to be 90%, 83%, and 79% viable respectively, after incubation for 48 h at 200 μM, indicating that thiol-specific effects are not a result of compound toxicity. It is noteworthy that abrogation of MAL-II and PNA epitopes was observed at 100 μM, suggesting that **1** inhibits *O*-glycan elaboration efficiently with minimal cytotoxicity.

Jurkat Cells Carry Substantial Levels of Elaborated *O*-Glycans Whose Expression Is Specifically Inhibited by 1. For non-lectin based evidence, we isolated *O*-glycans from Jurkat cells and characterized them by MALDI-TOF/TOF mass spectrometry.[38] Mass spectra of permethylated *O*-glycans from untreated Jurkat cells clearly showed peaks at *m*/*z* 691.29, 895.34, and 1256.46 corresponding, respectively, to sialyl-Tn (disaccharide), sialyl-T (trisaccharide), and disialyl-T (tetrasaccharide) antigen structures (Figure 3A). Glycan structures were further confirmed by MS/MS on precursor ion *m*/*z* 895.34, which yielded daughter ions at *m*/*z* 398.127 (B-ion, sialyl), 520.226 (Y-ion, T-antigen), and 620.257 (C-ion, sialyl-Gal) (Figure 3B). MS/MS of precursor ion *m*/*z* 1256.46 yielded expected daughter ions at *m*/*z* 398.15 (B-ion, sialyl), 506.21 (YY-ion, T-antigen), 620.20 (C-ion, sialyl-Gal), 659.31 (Z-ion, sialyl-Tn), and 881.405 (Y-ion, sialyl-T—linear/branched) (Figure 3C). It is pertinent to emphasize here that these

dx.doi.org/10.1021/ja405189k | J. Am. Chem. Soc. 2013, 135, 14189−14197

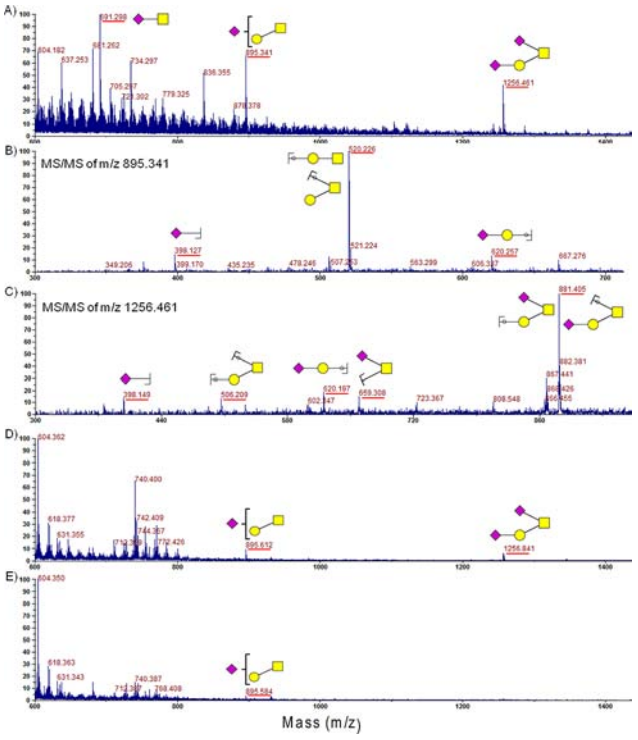

Figure 3. MALDI-TOF/TOF spectra revealed the presence of elaborated *O*-glycans in Jurkat cells and their suppression by **1**. Mass spectra of permethylated *O*-glycans from 35% acetonitrile in water fractions isolated from cells treated with (A) no vehicle, (D) **D**, and (E) **1** (100 μM, 48 h). MS/MS spectra of selected precursor ions from untreated cells corresponding to (B) sialyl-T and (C) disialyl-T structures. Relevant m/z peaks are underlined in red. Spectra shown are representative of at least two replicate samples. Monosaccharide symbols shown are as per the Consortium for Functional Glycomics (CFG) guidelines: Gal, yellow circle; GalNAc, yellow square; NeuAc, pink diamond.

structures have earlier been identified and characterized in CD43 isolated from Jurkat cells through radioactive labeling and chromatography.[34] Thus, based on MAL-II/PNA binding and mass spectrometry evidence, it can be concluded that Jurkat cells do express significant levels of elaborated *O*-glycans (notwithstanding *cosmc* mutation and reduced T-synthase activity).

A qualitative analysis of mass spectra revealed that cells treated with **D** showed *O*-glycan peaks similar to untreated cells (Figure 3D). However, cells incubated with **1** (100 μM, 48 h) showed the absence of disialyl-T (m/z 1256. 46) and the presence of very low levels of sialyl-T (m/z 895.34) *O*-glycans (Figure 3E), supporting abrogation of MAL-II epitopes. No evidence for the presence of GalNTGc could be obtained presumably due to levels of metabolic incorporation below the detection limit.

Ac_5GalNTGc (1) Drastically Alters Glycoforms of CD43 in a Dose- and Time-Dependent Manner. Having confirmed thiol-dependent global inhibition of elaboration of *O*-glycans induced by **1**, we focused on changes to glycoforms of selected cell surface antigens of immunological importance. CD43 was chosen as a model for mucin-type *O*-glycoproteins for the following reasons: (a) CD43 is heavily *O*-glycosylated with ~80−90 *O*-glycans (contributing 50−60% of total molecular weight) resulting in a bottle-brush-like structure for the extracellular domain,[39,40] (b) CD43 is known to be both a negative regulator and a coreceptor for immune activation,[7] and (c) glycoform-specific anti-CD43 antibody reagents were readily available. Jurkat cells express CD43 abundantly, and its *O*-glycans have been well characterized.[34,41] Three types of anti-CD43 antibodies, namely, *Neu*-sensitive (clones CD43-L60 and CD43-1G10), *Neu*-resistant (clone CD43-L10), and glycan-independent (clone CD43-C20, *C*-terminal), were employed (Figure 4A).[42] Cell surface estimation of CD43

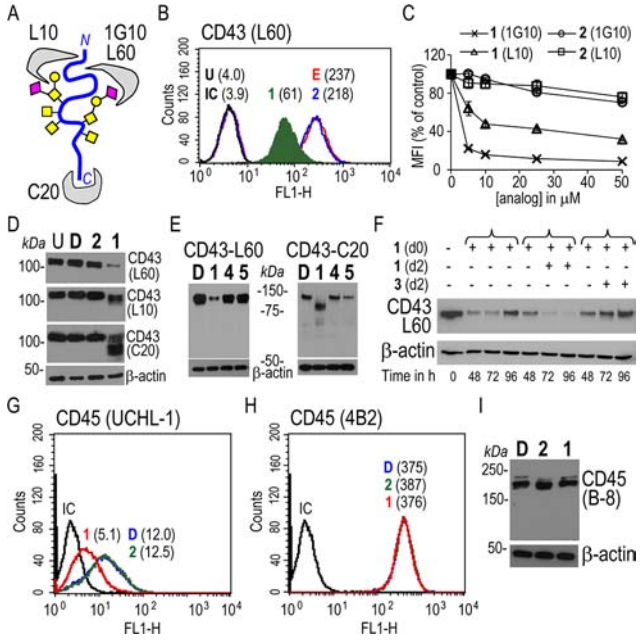

Figure 4. Glycoforms of CD43 and CD45 were altered by **1** in a thiol-specific and antigen-dependent manner in Jurkat cells. (A) Schematic representation of a CD43 glycoform showing binding epitopes of *Neu*-sensitive (clones 1G10 and L60), *Neu*-resistant (clone L10), and glycan-independent (*C*-terminal, clone C20) anti-CD43 antibodies. (B) Anti-CD43-L60 binding to cells after incubation with ethanol (E), **2**, or **1** (10 μM, 48 h). (C) Dose dependency of anti-CD43 (1G10 and L10) binding to cells treated with **1** or **2** (0 − 50 μM, 48 h) as measured by flow cytometry. (D) Anti-CD43 (L60, L10, and C20) Western blots of lysates of cells incubated with no vehicle (U), **D**, **2**, or **1** (100 μM, 48 h). (E) Anti-CD43 (L60 and C20) blots of cells incubated with **D**, **1**, **4**, or **5** (100 μM, 48 h). (F) Time course of CD43-L60 expression in lysates of cells treated with **1** (50 μM) for 48 h followed by treatment with **D**, **1**, or **3** (50 μM) at 48 h. Expression of CD45 (G) UCHL-1 (*Neu*-sensitive) and (H) 4B2 (*Neu*-resistant) epitopes in cells incubated with **D**, **2**, or **1** (10 μM, 48 h). (I) Anti-CD45 (B8, *C*-terminal, glycan-independent) Western blots of lysates of cells incubated with **D**, **2**, or **1** (100 μM, 48 h). MFI values in arbitrary units (a.u.) are shown in parentheses on histograms. Error bars shown are standard deviation of two replicate samples. Western blots shown are representative of at least two replicates with β-actin shown as loading control. *Neu*, neuraminidase; U, no antibody control; IC, isotype control; MFI, mean fluorescence intensity.

epitopes was performed under saturating antibody conditions (Supporting Information Figure S4). *Neu*-sensitive and *Neu*-resistant binding of CD43 antibodies were verified by flow cytometry (Supporting Information Figure S5).

Flow cytometry revealed that Jurkat cells do express abundant levels of CD43-L60 epitopes which were reduced to 26% of controls when incubated with **1**, but not **2** or vehicle (ethanol, **E**), at a low concentration of 10 μM for 48 h (MFI values of 237 and 218 a.u., respectively, for **E** and **2** compared

dx.doi.org/10.1021/ja405189k | J. Am. Chem. Soc. 2013, 135, 14189−14197

to 61 a.u. for **1**) (Figure 4B). A dose dependency study (0−50 μM, 48 h) with **1** showed drastic reduction in CD43-1G10 (15% of control at 50 μM) and significant reduction in CD43-L10 (50% of control at 50 μM) levels; in contrast, at 50 μM, both CD43-1G10 (95% of control) and CD43-L10 (90% of control) levels remained unaffected in cells treated with **2**, indicating thiol-specific interference in cell surface expression of CD43 glycoforms (Figure 4C).

In order to investigate changes to overall CD43 glycoforms, Western blotting was performed on total lysates from Jurkat cells incubated with no vehicle (untreated), **D**, **2**, or **1** (100 μM, 48 h) (Figure 4D). Specifically, treatment with **1** induced drastic reduction of CD43-L60 epitopes which appeared as sharp bands at 125 kDa in controls (U, **D**, and **2**). Similarly, significant reduction of CD43-L10 epitopes (along with appearance of multiple bands between 125 and 100 kDa) was induced specifically by **1**, but not U, **D**, or **2**, in agreement with flow cytometry results (Figure 4C). Strikingly, CD43-C20 blots revealed appearance of lower molecular weight bands in the range of 125−75 kDa, only in cells treated with **1**, but not U, **D**, or **2**. Clearly, treatment with **1** resulted in both hyposialylation (CD43-L60 and CD43-1G10) and hypoglycosylation (CD43-L10 and CD43-C20) of CD43 in a thiol-dependent manner. Further, treatment with analogues **4** and **5**—carrying acetylthio moiety with longer chain lengths—did not have the same effect as **1** on CD43 glycoforms indicating steric limitations on the thiol-specific effects (Figure 4E). A qPCR study of Jurkat cells incubated with **D**, **2** (200 μM), or **1** (10−200 μM) for 48 h revealed that CD43 mRNA levels remained unaffected (Supporting Information Figure S6). This confirmed that **1** interfered post-translationally in the glycosylation of CD43 resulting in appearance of multiple microheterogeneous glycoforms with lower molecular weights.

A time course study of CD43-L60 epitopes by Western blotting confirmed differential effects of **1** compared to **2** (Supporting Information Figure S7). To study reversibility of effects of **1** on CD43 glycosylation, Jurkat cells were first incubated with **D** or **1** (50 μM). After 48 h, cells were treated with **D**, another dose of **1** (50 μM), or **3** (50 μM). Cells were harvested at 48, 72, and 96 h and probed by Western blotting (Figure 4F). Cells treated with a single dose of **1** exhibited reduction in CD43-L60 levels up to 72 h but showed significant recovery by 96 h, whereas cells treated with two doses of **1** showed sustained reduction in CD43-L60 levels at 96 h. In the case of cells treated with **1** (at 0 h) followed by **3** (at 48 h), recovery of CD43-L60 levels was faster at 72 h and showed near-complete recovery by 96 h. Sustained suppression and recovery of CD43-L60 epitopes—using both non-natural and natural precursors—illustrate the facile flexibility of metabolic incorporation, dilution of non-natural metabolites with time, and restoration of wild-type glycosylation patterns. It is pertinent to emphasize here that effects observed with **1** in Jurkat cells are under competitive conditions wherein both GALE activity and UDP-GalNAc levels appear to be normal.[43] This is in contrast to earlier studies with **2** utilizing the mutant CHO-ldlD cell line that does not biosynthesize UDP-GalNAc endogenously.[21]

Ac_5GalNTGc (1) Alters Glycoforms Selectively in an Antigen-Dependent Manner. At the cellular level, apart from the metabolic processing of **1** and possible utilization of its metabolite UDP-GalNTGc as a donor by ppGalNAcTs, effects of **1** are likely to be governed by the nature of polypeptide acceptor substrates as well. This is likely to result in global, yet selective, effects of metabolic engineering. Thus for example CD45, another abundant protein on the T-cell surface, is known to carry only 8−17 *O*-glycans as opposed to 80−90 *O*-glycans on CD43.[41] To study susceptibility of other cluster of differentiation (CD) antigens to MGE, the effect of **1** on glycoforms of CD45 was probed using *Neu*-sensitive (clone CD45-UCHL-1), *Neu*-resistant (clone CD45-4B2), and glycan-independent (*C*-terminal, CD45-B8) antibodies. Incubation of Jurkat cells with **1** (10 μM, 48 h) caused significant reduction in CD45-UCHL-1 epitopes (MFI of 12 and 12.5 a.u for **D** and **2** respectively compared to 5.1 a.u. for **1**) (Figure 4G) while CD45-4B2 epitopes remained unchanged (MFI values of 375, 387, and 376 respectively for **D**, **2**, and **1**) (Figure 4H). Western blots using CD45-B8 revealed no significant change in the bands at 220 kDa upon treatment with either **D**, **2**, or **1** (100 μM, 48 h) (Figure 4I) in contrast to that observed with CD43-C20 (Figure 4D). It is quite possible that effects of **1** on CD45 are not reflected in Western blots due to counteracting factors of hyposialylation and hypoglycosylation. Also, the effect of **1** on *O*-glycans might be offset by a relatively large number of *N*-glycans present on CD45. By contrast, CD43 is known to carry only a single *N*-glycan site proximal to plasma membrane. These results illustrate global, yet selective, effects of metabolic engineering as a function of nature of cellular glycoprotein substrates.

Ac_5GalNTGc (1) Causes Drastic Hypoglycosylation of CD43 through Metabolic Incorporation. Having confirmed global—yet antigen-selective—thiol-dependent inhibition of *O*-glycan elaboration, we investigated whether GalNTGc was metabolically installed on CD43. A bioinformatics search revealed that CD43 was ideally suited for probing incorporation of GalNTGc *via* thiol-selective Michael addition reaction as it lacks "cysteine" in its polypeptide backbone. Therefore, susceptibility to thiol-selective ligation reactions could arise only due to the presence of GalNTGc. Indirectly, formation of UDP-GalNTGc from **1** and its ready utilization by ppGalNAcT was evident from earlier studies that showed an increase in CST levels.[26] In order to obtain direct evidence, we stably expressed CD43 carrying myc/FLAG tags at the *C*-terminus in Jurkat-E6.1 cells to facilitate immunoprecipitation in a glycan-independent manner (Supporting Information). CD43-L60 and anti-FLAG Western blots confirmed that thiol-specific effects of **1** were consistent in Jurkat-E6.1-CD43-myc/FLAG cells (Figure 5A) as observed with Jurkat cells (Figure 4D). Anti-FLAG blots showed characteristic bands at lower molecular weights (125−75 kDa) similar to CD43-C20. Cells were incubated with either **D** or **1** (100 μM, 48 h), and CD43-myc/FLAG was immunoprecipitated (Supporting Information Figure S8). Nontransfected and vector-transfected Jurkat-E6.1 cells were used as controls. CD43-myc/FLAG immunoprecipitates on beads were subjected to reduction by tris(2-carboxyethyl)phosphine hydrochloride (TCEP) followed by thiol-selective Michael addition using maleimide-PEG_2-biotin (MB) and analyzed by Western blotting (Figure 5B).[44] Strikingly, HRP-avidin blot revealed the presence of biotin exclusively on CD43-myc/FLAG immunoprecipitated from cells incubated with **1**, but not in controls. Anti-FLAG blot showed sharp bands at 125 kDa for vehicle-treated cells while cells treated with **1** showed characteristic diffuse bands from 125 to 75 kDa (a cross-reactive protein band at 125 kDa observed in silver stains and anti-FLAG blots was considered to be nonspecific as it eluted from nontransfected cells as well (Supporting Information Figure S8)). Notably, thiol-selective

dx.doi.org/10.1021/ja405189k | J. Am. Chem. Soc. 2013, 135, 14189−14197

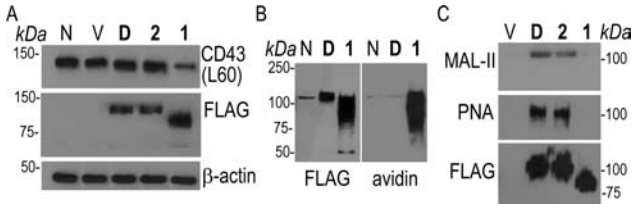

Figure 5. Abrogation of MAL-II and PNA epitopes on CD43 specifically through metabolic incorporation of **1**. (A) Anti-CD43-L60 and anti-FLAG Western blots of lysates of CD43-myc/FLAG stably transfected Jurkat-E6.1 cells incubated with **D**, **2**, or **1** (100 μM, 48 h). (B) Anti-FLAG and HRP-avidin blots of CD43-myc/FLAG immunoprecipitates from cells treated with **D** or **1** (100 μM, 48 h) subjected to TCEP treatment followed by MB. (C) Lectin blots using MAL-II and PNA of CD43-myc/FLAG immunoprecipitates from cells incubated with **D**, **2**, or **1** (100 μM, 48 h). For PNA, immunoprecipitates were subjected to *Neu* treatment prior to electrophoresis. β-Actin and anti-FLAG blots are shown as loading controls. Blots are representative of at least two replicates. *Neu*, neuraminidase; N, nontransfected; V, vector control; TCEP, tris(2-carboxyethyl)phosphine hydrochloride; MB, maleimide-PEG$_2$-biotin.

biotinylation was dependent upon prior reduction by TCEP indicating that most of the GalNTGc were spontaneously oxidized to disulfide forms on cell surface[18] and possibly during sample preparation (Supporting Information Figure S9). Thus, thiol-selective biotinylation of CD43-myc/FLAG confirmed direct metabolic incorporation of **1** as GalNTGc.

Additional proof of inhibition of elaboration of *O*-glycans on CD43 induced by **1** was obtained using lectin blots. CD43-myc/FLAG immunoprecipitates revealed the absence of MAL-II and PNA epitopes on CD43 upon treatment with **1**, but not **D** or **2** (Figure 5C), consistent with global effects observed by confocal microscopy, Western blots, and flow cytometry (Figures 2A, 2B, and 2C). Importantly, positive binding of MAL-II and PNA to CD43 from cells treated with **D** or **2** is in agreement with earlier work by Fukuda and others wherein CD43 isolated from Jurkat cells were found to carry both linear and branched sialyl-T and disialyl-T structures.[34] Probing for the effect of **D**, **2**, or **1** on Tn-epitopes on CD43-myc/FLAG immunoprecipitates using *Vivia villosa* agglutinin (VVA) and *Helix pomatia* agglutinin (HPA) revealed no major changes in binding, except for the lower molecular weight bands induced by **1** (Supporting Information Figure S10). Expectedly, *Neu* treatment increased binding of VVA and HPA in all three cases owing to increased accessibility of Tn structures. Therefore, based on lectin blots of CD43-myc/FLAG it might be concluded that metabolic incorporation of **1** does not seem to affect addition of initiating GalNAc residues to other S/T sites on CD43, but clearly abrogates elaboration by T-synthase and sialyltransferases.

Interestingly, ppGalNAcTs possess a ricin-like lectin domain that helps in anchoring a pre-existing GalNAc. Relative distance between active site and lectin domain is thought to determine the choice of neighbor site for addition of GalNAc.[45] Also, ppGalNAcTs prefer glycopeptides over peptides as substrates and exhibit unique site selectivities.[6,46] Speculatively, it is plausible that metabolic incorporation of **1** as GalNTGc on mucin-type *O*-glycoproteins modulates binding to lectin domain of ppGalNAcTs. This in turn might affect subsequent decoration of adjacent sites resulting in reduced site occupancy reflected in microheterogeneous lower molecular weight glycoforms. It is also known that ppGalNAcTs exhibit two free *Cys* side chains that form hydrogen bonds to UDP-GalNAc.[47] The sulfhydryl groups at the donor binding site could potentially interact with UDP-GalNTGc through redox mechanisms—possibly in an isoform selective manner—thus modulating kinetics of ppGalNAcT and glycosylation of their respective polypeptide acceptor substrates.

Both Sulfhydryl and Galactosamine Moieties Are Critical for Mucin-Type *O*-Glycan Inhibition. Next, we explored the mechanistic significance of galactosamine and thiol moieties for inhibition of *O*-glycosylation on CD43. Flow cytometry revealed that Ac$_4$GalNMeTA (**6**)—wherein sulfur is capped with a stable methyl group—did not affect CD43-1G10 epitopes on Jurkat cells even at 100 μM, while **1** induced a drastic reduction at 10 μM (Figure 6A). Lack of activity of **6**

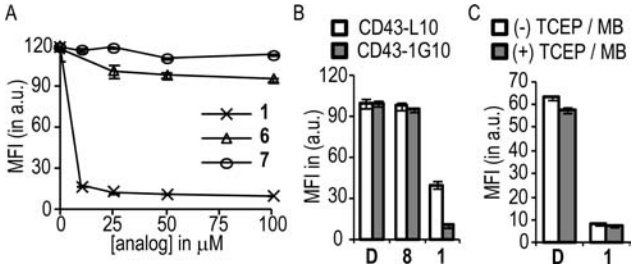

Figure 6. Both sulfhydryl and galactosamine moiety are critical for efficient inhibition of *O*-glycosylation of CD43 in Jurkat cells by **1**. (A) Flow cytometry estimation of anti-CD43-1G10 binding to cells incubated with **1**, **6**, or **7** (0–100 μM, 48 h). (B) Anti-CD43 (L10 and 1G10) binding to cells incubated with **D**, **8**, or **1** (100 μM, 48 h). (C) Anti-CD43-1G10 binding to cells incubated with **D** or **1** (100 μM, 48 h) followed by treatment with TCEP and MB. Error bars shown are standard deviation of two replicate samples. **D**, DMSO; *Neu*, neuraminidase, TCEP, tris(2-carboxyethyl)phosphine hydrochloride; MB, maleimide-PEG$_2$-biotin.

indicated that intracellular hydrolysis of acetylthio group to generate thiol from **1** is critical for inhibition. Similarly, Ac$_5$GlcNTGc (**7**)—the C-4 epimer of **1**—did not alter CD43-1G10 levels even at 100 μM (Figure 6A), suggesting that GlcNTGc is not readily converted to GalNTGc. Recent studies have shown that GALE could convert both GalNGc[21] and GalNAz[43] to GlcNGc and GlcNAz, respectively. However, efficiency of the reverse reaction is not known. The absence of activity with **7** suggests that GALE might not act upon GlcNTGc.

A strategy for inhibition of mucin-type *O*-glycan biosynthesis is through employment of substrate decoys that compete with glycoprotein substrates for glycosyl transferases.[11,12,48] A comparative flow cytometry study revealed that, unlike **1**, peracetylated *O*-Bn-α-GalNAc (**8**) did not change the levels of both CD43-1G10 and CD43-L10 epitopes. At 2.0 mM, the nonacetylated *O*-Bn-α-GalNAc (**9**) showed moderate reduction of CD43-1G10 and no change in CD43-L10 epitopes (Supporting Information Figure S11). This confirmed that **1** does not act by a substrate-decoy mechanism (Figure 6B). It is noteworthy that substrate decoys could affect only downstream of Tn-antigen, whereas **1** could potentially affect the biosynthesis of Tn-antigen by modulating ppGalNAcT action.

A possibility that lower molecular weight bands observed in anti-CD43-C20 blots could be a result of "hypersialylation" was ruled out as follows: Upon *Neu* treatment prior to lysis, as expected, CD43-L60 epitopes were reduced for **D** and **2**, and abrogated for **1**. In CD43-C20 blots, both **D** and **2** showed

dx.doi.org/10.1021/ja405189k | J. Am. Chem. Soc. 2013, 135, 14189–14197

characteristic bands at a higher apparent molecular weight due to loss of negatively charged sialic acids (Supporting Information Figure S12). By contrast, cells incubated with **1** showed no change upon *Neu* treatment confirming severe hypoglycosylation of CD43.

In principle, binding of antibodies to cell surface epitopes could be altered due to oligomerization of glycoproteins mediated by disulfides involving GalNTGc. To test if anti-CD43 binding is affected by MGE, Jurkat cells were incubated with **D** or **1** (100 μM, 48 h), followed by reduction of cell surface disulfides using TCEP, and capping of thiols using MB (Figure 6C). CD43-1G10 binding remained unaffected even after reduction and capping confirming that the observed thiol-specific effects are indeed due to hypoglycosylation of CD43. Similar results were observed for PNA binding as well (Supporting Information Figure S2).

CD43 Glycoforms Are Modulated Differentially by 1 in Hematopoietic Cells. Effects of metabolic processing of non-natural hexosamine analogues on cell surface glycoforms are governed by (a) specific chemical structure and reactivity of the non-natural moiety, (b) affinity of glycosyl transferases to activated non-natural sugar nucleotide donors, (c) expression and activity of multiple isoforms of each type of glycosyl transferases, and (d) nature and properties of acceptor polypeptide substrates. Expression of glycosylation machinery does vary widely among various cell types and also within a given cell type depending on whether it is activated or not.[49,50] Hence, in order to test if effects observed with **1** are general, we studied a panel of hematopoietic cell lines using changes to CD43 glycoforms as a read-out sensor. Flow cytometry revealed that treatment with **1** reduced binding of anti-CD43-L60 in all four cell lines indicating hyposialylation of CD43, albeit to different extents. Upon incubation with **1** (100 μM, 48 h), CD43-L60 levels were reduced to 11%, 31%, 42%, and 50% of untreated controls, respectively, in Jurkat, THP-1 (human acute monocytic leukemia), K562, and HL60 cells (Figure 7A).

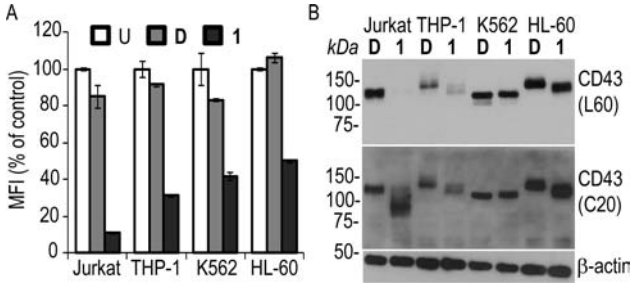

Figure 7. Thiol-dependent effects on CD43 glycoforms induced by **1** in various human cell lines. (A) Flow cytometry estimation of anti-CD43-L60 binding in Jurkat, THP-1, K562, and HL-60 cells incubated with no vehicle (U), **D**, or **1** (100 μM, 48 h). (B) Anti-CD43 (L60 and C20) Western blots of lysates of cells incubated with **D** or **1** (100 μM, 48 h). Error bars shown are standard deviation of two replicate samples. Western blots are representative of at least two replicates with β-actin shown as loading control. **D**, DMSO.

Cells treated with **D** did not show significant changes compared to untreated controls. Western blots using both anti-CD43-L60 and anti-CD43-C20 for vehicle treated cells showed bands at 125 kDa for Jurkat and K562, while THP-1 and HL-60 were observed at 130 kDa highlighting inherent variations among cell lines.[49] Treatment with **1** induced abrogation of CD43-L60 in Jurkat and THP-1, mild reduction in K562, and mild reduction with lower apparent molecular weights in HL60 cells. Corresponding anti-CD43-C20 blots showed lower molecular weight bands maximally for Jurkat, moderately for THP-1 and HL-60, and minimally for K562 cells induced by **1** (Figure 7B).

Differential effects of **1** and a threshold requirement for modulation of glycoforms among hematopoietic cell lines could be attributed to inherent load of glycans on CD43. For instance, mucin-type *O*-glycans of CD43 isolated from Jurkat cells carry ~83% of GalNAc and ~17% of elaborated *O*-glycans,[34] which is almost reversed in the case of CD43 from K562 cells, i.e. ~5% of GalNAc and ~95% of elaborated *O*-glycans.[36] Moderate effects of **1** on CD43-L60 in K562 compared to acute effects in Jurkat could, at least in part, be explained by robust T-synthase activity in K562 which is deficient in Jurkat.[34] Global effects at a cellular level would also be governed by differential expression, activity, and preference (or the lack thereof) for UDP-GalNTGc by the fourteen known human isoforms of ppGalNAcTs in various cell lines. Differential effects of **1** open up an interesting possibility of exploiting cell-type selective effects to modulate migration, trafficking, and behavior of leukocytes *via* modulation of glycoforms of cell surface antigens under disease conditions.

■ CONCLUSIONS

Our studies clearly show that effects of metabolic processing of non-natural GalNAc analogues in mammalian cells are governed by the chemical structure of functional groups and the nature of cellular protein substrates. Expression of MAL-II and PNA epitopes on Jurkat cells was abrogated in a thiol-specific manner by **1**. Glycoform-specific antibodies revealed drastic hypoglycosylation of CD43 induced specifically by **1**, but not **2**–**9**. Both thiol and galactosamine moieties of **1** were found to be critical for activity. Metabolic incorporation of **1** was established *via* thiol-selective biotinylation of CD43-myc/FLAG. Lectin blots of CD43 immunoprecipitates showed the absence of both MAL-II and PNA epitopes while HPA/VVA epitopes were unaffected. Glycoforms of CD43 and CD45 were altered differentially by **1** and found to be a function of polypeptide backbone and glycan load. Differential sensitivity of hematopoietic cells to **1** could be attributed to inherent differences in glycan load and glycosylation machinery. Considering that cell surface glycans, particularly on CD43, govern leukocyte trafficking in both immunity and autoimmune diseases,[51] it would be interesting to test if effects observed with **1** are translated *in vivo*. Ability to modulate glycan patterns in a selective set of immune cells using carbohydrate-based small molecules may open up new avenues for understanding biological functions of glycans in immunity, autoimmune diseases, and cancer.

■ EXPERIMENTAL PROCEDURES

Chemical Synthesis. Peracetylated non-natural GalNAc analogues **1**,[26] **2**,[21] **3**, **7**,[26] and **8**[27] were synthesized following the literature. Analogues **4**, **5**, and **6** were synthesized by analogous procedures, details of which are available in the Supporting Information.

Cell Culture, Antibodies, Lectins, Enzymes, and Reagents. Standard conditions used for mammalian cell culture are given in the Supporting Information. The following anti-human antibodies were employed in this study: anti-CD43 (FITC-1G10, FITC-L10, and L60) (BD Biosciences); goat polyclonal anti-CD43 (C-20) and anti-CD45 (B-8) (Santa Cruz Biotechnology); anti-CD45 (UCHL-1), polyclonal anti-FLAG, and anti-β-actin (AC-15) (Sigma-Aldrich). Purified anti-CD45 (clone 4B2) was a kind gift from Dr. A. Qadri (NII). Appropriate FITC and HRP-conjugated secondary and isotype control

antibodies were employed. Normal chicken serum (GIBCO) was a kind gift from Dr. V. K. Nandicoori (NII). Biotinylated lectins—bSNA, bMAL-II, bPNA, and bVVA—were obtained from Vector Laboratories, U.K. AlexaFluor488-HPA was obtained from Life Technologies. Neuraminidases from *Vibrio cholerae* and *Arthrobacter ureafaciens* (Roche), and from *Salmonella typhimurium* LT2 expressed in *Escherichia coli* (New England Biolabs (NEB)), were employed. PNGase-F was purchased from NEB. CD43-myc/FLAG plasmid was obtained from Origene and transfected using DMRIE-C (Life Technologies). MB was obtained from ThermoFisher Scientific. Anti-FLAG-M2-agarose beads, 3×FLAG peptide, and gelatin were purchased from Sigma-Aldrich.

Confocal Imaging of Lectin Stained Jurkat Cells. For washing of suspension-grown Jurkat cells, PBS containing $CaCl_2$ and $MgCl_2$ was used throughout in order to facilitate attachment to poly-L-lysine coated coverslips. Jurkat cells (3.0×10^5 cells/mL) in complete medium were incubated with either **D**, **1**, or **2** (100 μM). After 48 h, cells were collected, washed with PBS (2 × 1.0 mL), resuspended in PBS (400 μL), placed on coverslips (precoated with poly-L-lysine), and incubated at 37 °C. After 30 min, cells were gently washed with PBS (2 × 1.0 mL) and fixed with 2.0% formaldehyde (20 min, 22 °C), followed by washing with PBS (3 × 1.0 mL). For sialidase treatment, cells attached to coverslips were incubated with sialidase (0.005 unit per coverslip) from *Arthrobacter ureafaciens* in acetate buffer (pH 5.0) for 30 min at 37 °C, followed by washing with PBS (2 × 1.0 mL). Attached cells were blocked with 2.0% gelatin (Sigma-Aldrich) (30 min, 22 °C), washed with PBS (2 × 1.0 mL), and incubated with respective biotinylated lectin (30 min, 22 °C). Lectins were used at a concentration of 10 μg/mL in PBS for bSNA and bMAL-II; bPNA was diluted in a buffer containing 10 mM HEPES, pH 7.5, 0.15 M NaCl, 0.1 mM $CaCl_2$ as per suppliers' instructions. Cells were washed with PBS (3 × 1.0 mL), incubated with AlexaFluor-594 streptavidin conjugate (1:1000 dilution of 1.0 mg/mL stock solution) containing DAPI (1.0 μg/mL) (30 min, 22 °C), and washed with PBS (3 × 1.0 mL). The coverslips were mounted on microscope slides using ProLong Gold antifade reagent (Life Technologies). Confocal imaging was performed using LSM 510 Meta laser scanning microscope (Carl Zeiss) on multiple field views and coverslips.

Evaluation of PNA Binding by Flow Cytometry. Jurkat cells incubated with no vehicle, **D**, **1**, or **3** (50 μM, 48 h) were harvested and washed twice with PBS. Cells (5.0×10^5 cells per sample) were incubated without and with α-(2→3)-neuraminidase (from *Salmonella typhimurium* LT2 expressed in *E. coli*, 20 units) in 100 μL of PBS at 37 °C in a water bath. After 30 min, cells were washed twice with ice-cold lectin staining buffer (LSB) (10 mM HEPES buffer, containing 150 mM sodium chloride, 0.1 mM calcium chloride, and 0.08% sodium azide). Cells were stained using biotin-PNA (5 μg/mL) in 300 μL of LSB for 30 min in ice followed by FITC-avidin (1:250 dilution) in avidin staining buffer (ASB) (PBS containing 5% FBS and 0.1% sodium azide). After 30 min, cells were washed in ASB (3 × 0.5 mL), resuspended in 400 μL of ASB containing propidium iodide (PI, 2.5 μg/mL), and analyzed by flow cytometry. Samples were prepared in duplicate, and each sample was counted twice. About 20,000 events were acquired per sample, and PNA binding was analyzed by gating on PI negative viable cell population.

Thiol-Selective Biotinylation of Immunoprecipitated CD43-myc/FLAG. CD43-myc/FLAG captured on beads was resuspended in PBS and treated with TCEP (1.0 mM) for 30 min at 4 °C, after which MB was added at a final concentration of 2.0 mM.[44] Beads were rotated at 4 °C for 2 h and washed five times with lysis buffer. Bound protein was released from beads either by adding 3×FLAG peptide at a final concentration of 150 ng/μL and incubating at 4 °C for 30 min on rotation or by boiling in 2× Lämmli buffer for 5 min at 100 °C. Eluates or supernatants were subjected to 7.5% SDS−PAGE followed by silver staining and Western blotting. Blots were probed with HRP-Avidin (1:40,000 in 3.0% BSA-PBS, 50 ng/mL final concentration), anti-FLAG (1:5000 in PBS containing 5.0% NFM, 160 ng/mL final concentration), or anti-CD43 L60 (1:10,000 in PBS containing 5.0% NFM, 50 ng/mL final concentration).

■ ASSOCIATED CONTENT

Ⓢ Supporting Information

Supporting results and discussion, figures, detailed experimental procedures for synthesis of analogues **1**−**8**, cell culture, flow cytometry, Western blotting, immunoprecipitation, qPCR, and mass spectrometry. This material is available free of charge via the Internet at http://pubs.acs.org.

■ AUTHOR INFORMATION

Corresponding Author

*gopalan@nii.ac.in

Notes

The authors declare no competing financial interest.

■ ACKNOWLEDGMENTS

Funding support from National Institute of Immunology (NII), Department of Science and Technology (DST) (SR/S5/OBP-66B/2008), and Department of Biotechnology (DBT) (BT/PR11052/BRB/10/631/2008), Government of India, is gratefully acknowledged. S.-G.S. was supported by the Ramalingaswami Fellowship of DBT. S.-G.S. is grateful to Dr. Anne Dell and the Glyco-TRIC program for training on glycan mass spectrometry. We thank Dr. Mark Jones (Case Western Reserve University, Cleveland, OH) and Dr. R. P. Roy (NII) for critical reading of the manuscript. We thank Mr. Sebanta Pokhrel, Mr. Mohd. Aslam, and Mr. Arnob Nandi for technical help.

■ REFERENCES

(1) Varki, A., Cummings, R. D., Esko, J. D., et al., Eds. *Essentials of Glycobiology*, 2nd ed.; Cold Spring Harbor Laboratory Press: Cold Spring Harbor, NY, 2009. Available from http://www.ncbi.nlm.nih.gov/books/NBK1908/.
(2) Hang, H. C.; Bertozzi, C. R. *Bioorg. Med. Chem.* **2005**, *13*, 5021.
(3) Jentoft, N. *Trends Biochem. Sci.* **1990**, *15*, 291.
(4) Bennett, E. P.; Mandel, U.; Clausen, H.; Gerken, T. A.; Fritz, T. A.; Tabak, L. A. *Glycobiology* **2012**, *22*, 736.
(5) Ju, T.; Otto, V. I.; Cummings, R. D. *Angew. Chem., Int. Ed.* **2011**, *50*, 1770.
(6) Gill, D. J.; Clausen, H.; Bard, F. *Trends Cell Biol.* **2011**, *21*, 149.
(7) Manjunath, N.; Correa, M.; Ardman, M.; Ardman, B. *Nature* **1995**, *377*, 535.
(8) Ohtsubo, K.; Marth, J. D. *Cell* **2006**, *126*, 855.
(9) Schjoldager, K. T.; Vakhrushev, S. Y.; Kong, Y.; Steentoft, C.; Nudelman, A. S.; Pedersen, N. B.; Wandall, H. H.; Mandel, U.; Bennett, E. P.; Levery, S. B.; Clausen, H. *Proc. Natl. Acad. Sci. U.S.A.* **2012**, *109*, 9893.
(10) Tarp, M. A.; Clausen, H. *Biochim. Biophys. Acta* **2008**, *1780*, 546.
(11) Kuan, S. F.; Byrd, J. C.; Basbaum, C.; Kim, Y. S. *J. Biol. Chem.* **1989**, *264*, 19271.
(12) Sarkar, A. K.; Fritz, T. A.; Taylor, W. H.; Esko, J. D. *Proc. Natl. Acad. Sci. U.S.A.* **1995**, *92*, 3323.
(13) Hang, H. C.; Yu, C.; Ten Hagen, K. G.; Tian, E.; Winans, K. A.; Tabak, L. A.; Bertozzi, C. R. *Chem. Biol.* **2004**, *11*, 337.
(14) Sletten, E. M.; Bertozzi, C. R. *Angew. Chem., Int. Ed.* **2009**, *48*, 6974.
(15) Kayser, H.; Zeitler, R.; Kannicht, C.; Grunow, D.; Nuck, R.; Reutter, W. *J. Biol. Chem.* **1992**, *267*, 16934.
(16) Campbell, C. T.; Sampathkumar, S. G.; Yarema, K. J. *Mol. Biosyst.* **2007**, *3*, 187.
(17) Prescher, J. A.; Bertozzi, C. R. *Cell* **2006**, *126*, 851.
(18) Sampathkumar, S. G.; Li, A. V.; Jones, M. B.; Sun, Z.; Yarema, K. J. *Nat. Chem. Biol.* **2006**, *2*, 149.
(19) Hang, H. C.; Yu, C.; Kato, D. L.; Bertozzi, C. R. *Proc. Natl. Acad. Sci. U.S.A.* **2003**, *100*, 14846.

(20) Dube, D. H.; Prescher, J. A.; Quang, C. N.; Bertozzi, C. R. *Proc. Natl. Acad. Sci. U.S.A.* **2006**, *103*, 4819.
(21) Bergfeld, A. K.; Pearce, O. M.; Diaz, S. L.; Lawrence, R.; Vocadlo, D. J.; Choudhury, B.; Esko, J. D.; Varki, A. *J. Biol. Chem.* **2012**, *287*, 28898.
(22) Hang, H. C.; Yu, C.; Pratt, M. R.; Bertozzi, C. R. *J. Am. Chem. Soc.* **2004**, *126*, 6.
(23) Marathe, D. D.; Buffone, A., Jr.; Chandrasekaran, E. V.; Xue, J.; Locke, R. D.; Nasirikenari, M.; Lau, J. T.; Matta, K. L.; Neelamegham, S. *Blood* **2010**, *115*, 1303.
(24) Pouilly, S.; Bourgeaux, V.; Piller, F.; Piller, V. *ACS Chem. Biol.* **2012**, *7*, 753.
(25) Pouilly, S.; Piller, V.; Piller, F. *FEBS J.* **2012**, *279*, 586.
(26) Du, J.; Che, P. L.; Aich, U.; Tan, E.; Kim, H. J.; Sampathkumar, S. G.; Yarema, K. J. *Bioorg. Med. Chem. Lett.* **2011**, *21*, 4980.
(27) Paulsen, H.; Volker, P.; Brockhausen, I. *Liebigs Ann. Chem.* **1992**, *5*, 513.
(28) Keppler, O. T.; Horstkorte, R.; Pawlita, M.; Schmidt, C.; Reutter, W. *Glycobiology* **2001**, *11*, 11R.
(29) Rillahan, C. D.; Antonopoulos, A.; Lefort, C. T.; Sonon, R.; Azadi, P.; Ley, K.; Dell, A.; Haslam, S. M.; Paulson, J. C. *Nat. Chem. Biol.* **2012**, *8*, 661.
(30) Nishimura, S.; Hato, M.; Hyugaji, S.; Feng, F.; Amano, M. *Angew. Chem., Int. Ed.* **2012**, *51*, 3386.
(31) Barthel, S. R.; Antonopoulos, A.; Cedeno-Laurent, F.; Schaffer, L.; Hernandez, G.; Patil, S. A.; North, S. J.; Dell, A.; Matta, K. L.; Neelamegham, S.; Haslam, S. M.; Dimitroff, C. J. *J. Biol. Chem.* **2011**, *286*, 21717.
(32) Zandberg, W. F.; Kumarasamy, J.; Pinto, B. M.; Vocadlo, D. J. *J. Biol. Chem.* **2012**, *287*, 40021.
(33) Gupta, G.; Surolia, A.; Sampathkumar, S. G. *OMICS* **2010**, *14*, 419.
(34) Piller, V.; Piller, F.; Fukuda, M. *J. Biol. Chem.* **1990**, *265*, 9264.
(35) Wilkins, P. P.; McEver, R. P.; Cummings, R. D. *J. Biol. Chem.* **1996**, *271*, 18732.
(36) Maemura, K.; Fukuda, M. *J. Biol. Chem.* **1992**, *267*, 24379.
(37) Ju, T.; Lanneau, G. S.; Gautam, T.; Wang, Y.; Xia, B.; Stowell, S. R.; Willard, M. T.; Wang, W.; Xia, J. Y.; Zuna, R. E.; Laszik, Z.; Benbrook, D. M.; Hanigan, M. H.; Cummings, R. D. *Cancer Res.* **2008**, *68*, 1636.
(38) Sutton-Smith, M.; Dell, A. In *Cell Biology*; 3rd ed.; Celis, S., Ed.; Academic Press: 2006; Vol. *4*, p 415.
(39) Fukuda, M.; Tsuboi, S. *Biochim. Biophys. Acta* **1999**, *1455*, 205.
(40) Cyster, J. G.; Shotton, D. M.; Williams, A. F. *EMBO J.* **1991**, *10*, 893.
(41) Clark, M. C.; Baum, L. G. *Ann. N.Y. Acad. Sci.* **2012**, *1253*, 58.
(42) Weber, S.; Ruh, B.; Dippel, E.; Czarnetzki, B. M. *Immunology* **1994**, *82*, 638.
(43) Boyce, M.; Carrico, I. S.; Ganguli, A. S.; Yu, S. H.; Hangauer, M. J.; Hubbard, S. C.; Kohler, J. J.; Bertozzi, C. R. *Proc. Natl. Acad. Sci. U.S.A.* **2011**, *108*, 3141.
(44) Sampathkumar, S. G.; Li, A. V.; Yarema, K. J. *Nat. Protoc.* **2006**, *1*, 2377.
(45) Fritz, T. A.; Hurley, J. H.; Trinh, L. B.; Shiloach, J.; Tabak, L. A. *Proc. Natl. Acad. Sci. U.S.A.* **2004**, *101*, 15307.
(46) Pratt, M. R.; Hang, H. C.; Ten Hagen, K. G.; Rarick, J.; Gerken, T. A.; Tabak, L. A.; Bertozzi, C. R. *Chem. Biol.* **2004**, *11*, 1009.
(47) Tenno, M.; Toba, S.; Kezdy, F. J.; Elhammer, A. P.; Kurosaka, A. *Eur. J. Biochem.* **2002**, *269*, 4308.
(48) Patsos, G.; Robbe-Masselot, C.; Klein, A.; Hebbe-Viton, V.; Martin, R. S.; Masselot, D.; Graessmann, M.; Paraskeva, C.; Gallagher, T.; Corfield, A. *Biochem. Soc. Trans.* **2007**, *35*, 1372.
(49) Carlsson, S. R.; Fukuda, M. *J. Biol. Chem.* **1986**, *261*, 12779.
(50) Piller, F.; Piller, V.; Fox, R. I.; Fukuda, M. *J. Biol. Chem.* **1988**, *263*, 15146.
(51) Ford, M. L.; Onami, T. M.; Sperling, A. I.; Ahmed, R.; Evavold, B. D. *J. Immunol.* **2003**, *171*, 6527.